

Structural Basis for Cold Adaptation

SEQUENCE, BIOCHEMICAL PROPERTIES, AND CRYSTAL STRUCTURE OF MALATE DEHYDROGENASE FROM A PSYCHROPHILE *AQUASPIRILLIUM ARCTICUM**

(Received for publication, December 23, 1998, and in revised form, February 5, 1999)

Sun-Yong Kim, Kwang Yeon Hwang, Sung-Hou Kim‡, Ha-Chin Sung§, Ye Sun Han, and Yunje Cho¶

From the Structural Biology Center, Korea Institute of Science and Technology, P.O. Box 131, Cheongryang, Seoul 130-650, South Korea, the §Department of Biotechnology, Korea University, and the ‡Department of Chemistry and E. O. Lawrence Berkeley National Laboratory, University of California, Berkeley, California 94720

***Aquaspirillum arcticum* is a psychrophilic bacterium that was isolated from arctic sediment and grows optimally at 4 °C. We have cloned, purified, and characterized malate dehydrogenase from *A. arcticum* (Aa MDH). We also have determined the crystal structures of apo-Aa MDH, Aa MDH-NADH binary complex, and Aa MDH-NAD-oxaloacetate ternary complex at 1.9-, 2.1-, and 2.5-Å resolutions, respectively. The Aa MDH sequence is most closely related to the sequence of a thermophilic MDH from *Thermus flavus* (Tf MDH), showing 61% sequence identity and over 90% sequence similarity. Stability studies show that Aa MDH has a half-life of 10 min at 55 °C, whereas Tf MDH is fully active at 90 °C for 1 h. Aa MDH shows 2–3-fold higher catalytic efficiency compared with a mesophilic or a thermophilic MDH at the temperature range 4–10 °C. Structural comparison of Aa MDH and Tf MDH suggests that the increased relative flexibility of active site residues, favorable surface charge distribution for substrate and cofactor, and the reduced intersubunit ion pair interactions may be the major factors for the efficient catalytic activity of Aa MDH at low temperatures.**

Psychrophiles grow at low temperatures, where most of other organisms cannot grow. In order to survive such extreme environments (less than 4 °C), enzymes from psychrophiles must catalyze efficiently at low temperatures (1–6). While good progress is being made to elucidate the adaptation mechanism of enzymes from some extremophiles including hyperthermophile, the molecular basis of cold adaptation of psychrophilic enzymes is relatively poorly understood (7–9). However, psychrophilic enzymes have generated considerable interest, since they can be used to improve the efficiency of industrial processes and for environmental applications (1, 10). Also, comparison of the structures of psychrophilic enzymes with mesophilic, thermophilic, and hyperthermophilic counterparts may

add new insights into the understanding of catalytic mechanism and analysis of thermostability factors.

As a first step to understand the structural basis of cold adaptation of psychrophilic enzymes, we have carried out biochemical and structural studies of malate dehydrogenase from *Aquaspirillum arcticum*, a psychrophilic bacterium that was isolated from Arctic sediments and grows optimally at 4 °C (11).

MDH¹ is a homodimeric enzyme that catalyzes the reversible oxidation of malate to oxaloacetate in the presence of NAD in the citric acid cycle and thus plays a major role in central metabolism (12). Therefore, a certain amount of MDH is always expected to be present in most living organisms. Several MDHs from different sources have been extensively studied in genetic and biochemical aspects; sequences of a large number of malate dehydrogenases from organisms representing Archea, Bacteria, and Eukarya have been reported, and many of their gene products have been characterized. Furthermore, crystal structures of MDHs from the thermophile *Thermus flavus* (13), the mesophile *Escherichia coli* (14, 15), porcine heart mitochondria (16), and cytoplasm (17) have been determined.

Recently, a few psychrophilic enzymes including subtilisin from *Bacillus* TA41 (3), amylase from *Alteromonas haloplantidis* A23 (4), citrate synthase from DS2-3R (5), and alcohol dehydrogenase from *Moraxella* sp. TAE123 (6) have been isolated, and their characteristics have been compared with mesophilic or thermophilic counterparts. The commonly observed biochemical features of these cold active enzymes are (i) their increased catalytic efficiencies at low temperatures and (ii) significantly increased thermostability compared with mesophilic or thermophilic counterparts. However, it is difficult to understand the properties of cold active enzymes at the molecular level from the studies described above, since most of these studies were carried out in the absence of structures of psychrophilic enzymes.

In the present study, we have cloned a MDH gene from *A. arcticum* and purified and characterized its product. We also report here the high resolution crystal structures of apo-Aa MDH, Aa MDH-NADH binary complex, and Aa MDH-NAD-oxaloacetate ternary complex (Table I) and describe our analysis of how psychrophilic MDH may catalyze efficiently at low temperatures.

EXPERIMENTAL PROCEDURES

Purification—Four liters of *A. arcticum* cells, obtained from DSM, were grown in tryptic soy broth (Difco) at 4 °C for 3–4 days. Cells were

* This work was supported by the MOST Biotech 2000 program, the Korea Institute of Science and Technology KIST 2000 program, and the U.S. Department of Energy. The costs of publication of this article were defrayed in part by the payment of page charges. This article must therefore be hereby marked "advertisement" in accordance with 18 U.S.C. Section 1734 solely to indicate this fact.

The nucleotide sequence(s) reported in this paper has been submitted to the GenBank™/EBI Data Bank with accession number(s) AF109682.

The coordinates and structure factors (accession codes: 1b8p for apo-Aa MDH, 1b8v for Aa MDH-NADH, and 1b8u for Aa MDH-NAD-OAA) have been deposited in the Protein Data Bank, Brookhaven National Laboratory, Upton, NY.

¶ Supported by a KAST young scientist award in life science. To whom correspondence should be addressed. Tel.: 822-958-5937; Fax: 822-958-5939; E-mail: yunje@sbc4.kist.re.kr.

¹ The abbreviations used are: r.m.s., root mean square; MDH, malate dehydrogenase; Aa MDH, *A. arcticum* malate dehydrogenase; Tf MDH, *T. flavus* malate dehydrogenase; Ec MDH, *E. coli* malate dehydrogenase.

harvested and resuspended in 100 mM of Tris-Cl, pH 8.2, buffer containing 0.5 mM phenylmethylsulfonyl chloride. The cells were lysed in a French press, and the insoluble debris was removed by centrifugation. The supernatant was loaded to a Q-Sepharose column equilibrated with 50 mM Tris-HCl (pH 8.2). Fractions containing MDH were eluted between 0.4 and 0.5 M NaCl. These fractions were pooled, concentrated using ultrafiltration, and applied to a Blue Sepharose CL-6B column preequilibrated with same buffer. Aa MDH was eluted with 2 mM NADH. The protein was further purified by a size exclusion column (Superdex 75). SDS-polyacrylamide gel electrophoresis analysis of the final preparation showed a single band of protein with 95% homogeneity.

Cloning—Trypsin digestion of a purified Aa MDH results in two fragments with approximate molecular mass of 27 and 9 kDa. N-terminal sequencing of intact Aa MDH and a fragment corresponding to 27 kDa provides the sequences AKTPMRVAVTGAAGQLXYSLL and XDLXIXXQIFTVQGXAXDAVA, respectively. Two degenerate oligomers were derived from these sequences, and polymerase chain reaction was performed using these primers and genomic DNA from *A. arcticum* as a template. The polymerase chain reaction resulted in a major single product with the expected size and several nonspecific products.

The genomic DNA was digested by several restriction enzymes, blotted onto a Hybond-N+ membrane, and analyzed by Southern hybridization using the polymerase chain reaction-amplified product as a probe. A 2.4-kb *Hind*III fragment that hybridized to the polymerase chain reaction product was isolated, ligated with pBluescript KS(+), and transformed into *E. coli* DH5 α . Sequencing of this plasmid confirmed the presence of a complete Aa MDH gene.

Kinetics and Thermostability Measurements—Kinetic parameters were determined for Aa MDH, Tf MDH (Sigma), and MDH from *E. coli* (Ec MDH; Sigma). Reaction mixtures containing 100 mM Tris-HCl (pH 7.5), 500 μ M oxaloacetate, and enzyme were incubated at 4, 10, and 37 °C. The NADH (5–200 μ M final concentration) were added to the mixture, and the amount of NAD produced was measured at various temperatures and times. K_m and k_{cat} values were determined by Lineweaver-Burk plots using the ENZFITTER (18) data analysis program.

Thermostability was measured for Aa MDH, Ec MDH, and Tf MDH in buffer containing 100 mM Tris-HCl, 500 μ M oxaloacetate, 100 μ M NADH, pH 7.5. Each enzyme was incubated at 55 °C for various times and then cooled on ice. The residual enzyme activity was measured with 500 μ M oxaloacetate and 100 μ M NADH at 37 °C using the standard protocol described above.

Crystallization—The enzyme was dialyzed against 50 mM Tris-HCl, pH 8.2, 100 mM NaCl. Equal volumes of protein (10 mg/ml) and reservoir solution (100 mM Tris-HCl, 400 mM sodium acetate, 35% polyethylene glycol 4000, pH 8.0) were mixed and equilibrated with 1 ml of reservoir solution at 18 °C using the hanging drop vapor diffusion method. Crystals with a size of 0.2 \times 0.2 \times 0.3 mm appeared within 4–10 days. NADH binding was carried out by transferring the crystal to a reservoir solution containing 100 mM NADH for 2 days. To make the ternary complex, the crystal was initially soaked in reservoir solution containing 100 mM NAD for 2 days, and then oxaloacetate was added to a final concentration of 200 mM and incubated at 18 °C for 36 h. x-ray diffraction data were measured to 1.9 Å for the apo-Aa MDH, 2.1 Å for the binary complex, and 2.5 Å for the ternary complex. All data were measured on a Mar30 image plate system mounted on a Rigaku RU-200 rotating anode x-ray generator. Data for the apo-Aa MDH and binary complex were measured at 18 °C, whereas the data for the ternary complex were collected at –190 °C using a flash frozen crystal. Determination of unit cell parameters and integration of reflections was performed using the program DENZO (19) from the HKL package. Data were scaled and merged with SCALEPACK (19).

Refinement and Model Building—The structure of the apoenzyme was solved by the molecular replacement method as implemented in X-PLOR (20) using a search model built from Tf MDH, where side chains of nonidentical residues were replaced by alanine or glycine and the portions with inserted or deleted regions were removed. Rotation and translation functions of the method gave a unanimous solution; the highest peak from the translation search in the resolution range of 15–4 Å was 3 times higher than the mean value. The initial R-factor was 48.15%. One round of rigid body refinement dropped the R-factor to 29.7% in the resolution range of 10–4 Å. With a correctly positioned model, $|F_o| - |F_c|$ and $2|F_o| - |F_c|$ maps were calculated, and manual adjustment of the model was performed using the program CHAIN (21). The model was further refined using X-PLOR with Engh and Huber stereochemical parameters (22). Refinement statistics are presented in Table I. Because the first two N-terminal residues are not clearly defined, they are not included in the final model. The final models

TABLE I
Diffraction data and refinement statistics

	Aa MDH	Aa MDH · NADH	Aa MDH · NAD · OAA
Space group	P2 ₁ 2 ₁ 2	P2 ₁ 2 ₁ 2	P2 ₁ 2 ₁ 2
Cell dimensions (Å)			
<i>a</i>	58.97	59.02	58.30
<i>b</i>	102.24	102.52	101.70
<i>c</i>	53.69	53.96	52.76
Total observations	97,406	42,769	68,254
Unique reflections >2 σ	23,657	15,700	9273
R_{sym} (%) ^a	8.1	7.4	7.5
R_{cryst} (%)	17.4	18.3	19.8
R_{free} (%) ^b	17.8	20.8	23.4
Resolution (Å)	8.0–1.9	8.0–2.1	8.0–2.5
r.m.s. bonds (Å) ^c	0.009	0.008	0.010
r.m.s. angles (degrees) ^c	1.45	1.51	1.65

^a $R_{sym} = \sum_h \sum_i |I_{h,i} - I_h| / \sum_h \sum_i I_{h,i}$ for the intensity (I) of i observations of reflection h .

^b 10% of total reflections were set aside to calculate the R_{free} value.

^c Root mean square deviations from ideal geometry.

contain 327 residues and 220 water molecules for apo-Aa MDH; 327 residues, 127 water molecules, and 1 NADH molecule for the binary complex; and 327 residues, 62 water molecules, 1 NAD molecule, and 1 oxaloacetate molecule for the ternary complex.

RESULTS AND DISCUSSION

Cloning and Sequence Comparison

Aa MDH is composed of 329 amino acids, and its sequence is most similar to those of Tf MDH (61% identity and over 90% similarity) among all available MDH sequences (Fig. 1a). Composition analysis shows that Aa MDH has slightly lower Arg/(Arg + Lys) content (43%) than Tf MDH (51%). While Glu (13 *versus* 24%) and Arg (13 *versus* 19%) contents in Tf MDH are significantly higher than those in Aa MDH, other charged residue contents are similar in two enzymes. The numbers of glycine (28 *versus* 27 for Aa MDH *versus* Tf MDH) and proline (16 *versus* 16) residues are very similar in the two proteins. While numbers of hydrophobic residues with the aromatic ring are equal in both MDH, some differences are observed in isoleucine (23 *versus* 17), valine (22 *versus* 27), and leucine (27 *versus* 30).

Kinetic and Stability Properties of Aa MDH

The kinetic constants were determined for MDHs from three species, a psychrophile, a mesophile, and a thermophile at three different temperatures, and are summarized in Table II. The k_{cat}/K_m of Aa MDH was approximately 2–3-fold higher than that of Ec MDH at 4–10 °C. The activities of Tf MDH at 4–10 °C were too low, and we could not measure the kinetic constant of Tf MDH at these temperatures within our limit. The k_{cat}/K_m values of Aa MDH and Ec MDH are almost equal at 37 °C.

For stability studies, each enzyme was preheated at various temperatures for a given time, and the activities were measured. The half-time of inactivation ($t_{1/2}$) of each MDH is shown in Table II. The activity of Aa MDH decreased to 50% at 55 °C for 10 min. The half-time of inactivation ($t_{1/2}$) of Ec MDH was 20 min at 55 °C, showing a 2-fold increase compared with Aa MDH. Tf MDH retains full activity at 55 °C for more than 2 h. It has been reported that Tf MDH is fully active after heating at 90 °C for 1 h (13). Circular dichroism measurement also shows a large difference of T_m values between Aa MDH (58 °C) and Tf MDH (>95 °C).

X-ray Structure

Overall Structure—We will focus on a structural comparison between psychrophilic Aa MDH and thermophilic Tf MDH throughout this study, since these two enzymes show remark-

TABLE II
Comparison of kinetic and thermolability parameters of three MDHs

Parameters	Aa MDH	Ec MDH	Tf MDH
Kinetics			
4 °C			
k_{cat} (s ⁻¹)	152 ± 22	93 ± 15	
K_m^{app} (μM)	16 ± 4	23 ± 5	ND ^a
$k_{\text{cat}}/K_m^{\text{app}}$	11	4	
10 °C			
k_{cat} (s ⁻¹)	277 ± 18	171 ± 18	
K_m^{app} (μM)	23 ± 4	26 ± 4	ND
$k_{\text{cat}}/K_m^{\text{app}}$	12	7	
37 °C			
k_{cat} (s ⁻¹)	1111 ± 150	1108 ± 290	419 ± 33
K_m^{app} (μM)	45 ± 10	56 ± 11	14 ± 4
$k_{\text{cat}}/K_m^{\text{app}}$	25	20	30
Thermolability			
$t_{1/2}$	10 min		>2 h
T_m	58 °C		>95 °C

^a ND, kinetic constants could not be determined because of low enzyme activity at these temperatures.

between α10 and β10, where the r.m.s. deviation value is 3.8 Å. Minor differences are observed in the loop between β2 and α2, where two more residues are inserted in Aa MDH. The Aa MDH and Ec MDH show more significant deviations (r.m.s. deviation of 2.4 Å for 256 C-α atoms), reflecting their low sequence identity of 27%.

NADH Binding Site—The presence of NADH in the NADH-soaked crystal was clearly identified from the simulated annealed omit map of NADH complex crystal (Fig. 2a). Comparisons between apo-Aa MDH and Aa MDH·NADH complex structures show an r.m.s. deviation of 0.31 Å, suggesting that NADH did not induce any noticeable conformational changes. The NADH is hydrogen-bonded to the side chains of Glu⁴³ (2.7, 2.9 Å), Gln¹¹⁵ (3.3 Å), Asn¹³⁴ (3.5 Å), and His¹⁹⁰ (3.0 Å) and main chain atoms of Gly¹² (3.2 Å), Gln¹⁶ (2.9 Å), Ile¹⁷ (2.9 Å), Val¹³² (3.0 Å), and Asn¹³⁴ (3.1 Å) (Fig. 2b). Most of the NADH binding residues are highly conserved both in Aa MDH and Tf MDH (Fig. 1a). However, the side chain of Gln¹⁴ of Tf MDH forms a hydrogen bond to the NO1 (3.3 Å) atom and AO-1 (3.1 Å) atom of NADH, whereas the side chain of a corresponding residue, Gln¹⁶ in Aa MDH points away from the NADH. These differences may contribute to the increased K_m of NADH in Aa MDH compared with that in Tf MDH at 37 °C.

It has been proposed that the surface loop formed by residues 90–100 plays an important role in the binding of NADH (13, 17). In lactate dehydrogenase, another NADH binding enzyme whose tertiary structure is similar to MDH, significant conformational changes in this loop occur upon binding of NADH (23, 24). While no direct evidence of such gross conformational changes within the surface loop has been observed in MDH, the compositions of the amino acids and the main chain atom positions in this region are very similar in both Aa MDH and Tf MDH.

Ternary Complex—MDH catalyzes an ordered reaction, where NADH binds first, followed by the dicarboxylic acid substrate (25). The substrate binding site was identified by first soaking the crystal in buffer containing NAD and later with oxaloacetate. The resulting omit map clearly reveals the presence of a NAD and a substrate (Fig. 3a). Although oxaloacetate binds near NAD, no direct interactions were observed between the two molecules. The C-4 atom of the nicotinamide moiety of NAD is 5.9 Å away from the C-2 atom of oxaloacetate, and a water molecule is present between the two atoms (Fig. 3b). Important residues involved in oxaloacetate binding include Arg¹⁶⁵ (2.6 and 3.2 Å), His¹⁹⁰ (3.1 Å), and Ser²⁴¹ (3.3 Å). The main chain atoms of Arg²²⁹ (3.5 Å) and Gly²³⁰ (2.9 Å) also

form hydrogen bonds to oxaloacetate (Fig. 3b). The carbonyl oxygen of Gly²²⁷ is 2.9 Å away from the O1A atom of oxaloacetate. Thus, it is possible that these two atoms may form a hydrogen bond if the O1A atom of oxaloacetate becomes protonated.

In lactate dehydrogenase, the C-4 atom of the nicotinamide ring in NADH and the C-2 atom of the substrate analogue, oxamate, are located closer (3.7 Å), such that the proton can be directly transferred to the C-2 atom of lactate from NADH (23, 24). Structure comparison reveals that the binding of substrate to LDH induces a gross conformational change (up to 14 Å) in the surface loop around the NADH binding region, which is equivalent to residues 89–100 in Aa MDH. However, the binding of oxaloacetate to Aa MDH did not induce any notable conformational changes as judged by comparison of the ternary complex structure with apo- and binary Aa MDH enzyme structures (r.m.s. deviation of 0.33 and 0.34 Å, respectively). Therefore, it is possible that the large conformational change upon oxaloacetate binding may be necessary to bring the substrate closer to NAD, and this structural rearrangement is limited inside the crystal due to the crystal packing. Thus far, no ternary complex structures of MDH from other organisms, substrate, and coenzyme have been reported. However, the ternary complex of Ec MDH, NAD, and substrate analogue (citrate) has been determined at 1.9-Å resolution, and the distance between the C-4 atom of the nicotinamide ring in NAD and the C-3 atom of citrate was 4.9 Å (15).

Comparison of the oxaloacetate binding site of Aa MDH and an equivalent region of Tf MDH reveals that all of the residues interacting with oxaloacetate are conserved except for Gly²²⁷, which has been replaced by alanine in Tf MDH. Since the main chain of glycine has more conformational freedom than any other amino acid, substitution of Gly²²⁷ in Aa MDH from Ala²²⁷ may provide more local flexibility in Aa MDH, and this may partly contribute to the high catalytic efficiency of Aa MDH at low temperatures.

Flexibility—It has been proposed that increased flexibility is the most important factor for the catalytic efficiency of psychrophilic enzymes at low temperatures (1, 2). The crystallographic thermal factors of the structures of Aa MDH and Tf MDH have been compared to analyze the flexibility of both enzymes. Aa MDH·NADH complex had an average B-factor of 15.10 Å² for main chain atoms, significantly lower than that of Tf MDH·NADH, 23.56 Å². Also, average B-factors for main chain atoms of each domain in Aa MDH (N-domain, 14.75 Å²; C-domain, 15.45 Å²) show similar differences compared with those in Tf MDH (N-domain, 23.14 Å²; C-domain, 24.03 Å²). However, differences in resolution, packing, solvent content, and quality of data could contribute to B-factors. To correlate the local flexibility of each MDH in an equivalent scale of thermal parameters, we have divided the B-factors of all atoms in each enzyme by an average B-factor of a whole molecule (termed relative B-factor) and compared these values for the two proteins (Fig. 4). All main chain atoms (Gly¹², Gln¹⁶, Ile¹⁷, Val¹³², Asn¹³⁴, Gly²²⁷, Arg²²⁹, Gly²³⁰) and most of the side chain atoms (Glu⁴³, Arg¹⁶⁵, Ser²⁴¹) interacting with NADH and oxaloacetate in Aa MDH had up to approximately 2-fold increased relative B-factors, reflecting their increased relative flexibility (Fig. 4). We have also used two different methods to compare the relative flexibility of the active site regions in both MDHs. First, the B-factors for the atoms of active site residues were divided by the average B-factors of the rest of the atoms in the whole molecule. This was to remove any bias resulting from the active site residues in local flexibility calculation. Second, the average B-factors for the whole molecule without the active site residues were subtracted from the B-factors for each of the

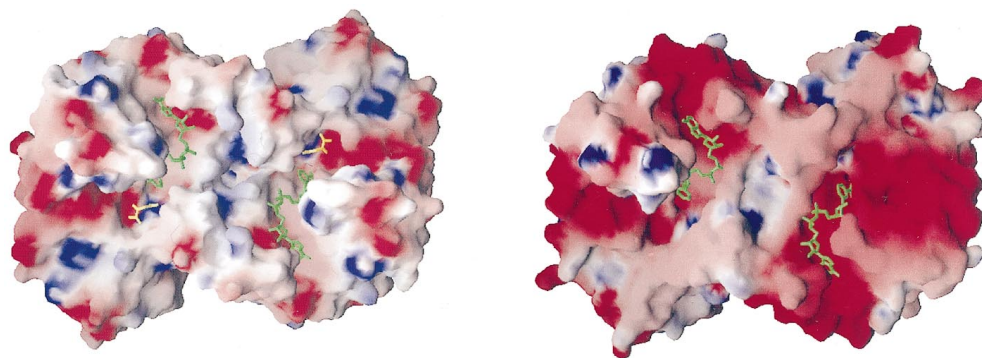


FIG. 5. Comparison of the electrostatic potential of Aa MDH (*left*) and Tf MDH (*right*). NADH is shown in *green*, and oxaloacetate is in *yellow*. The positive potential is in *blue*, and the negative potential is in *red*. The electrostatic potential is calculated for each molecule in the absence of NADH and oxaloacetate.

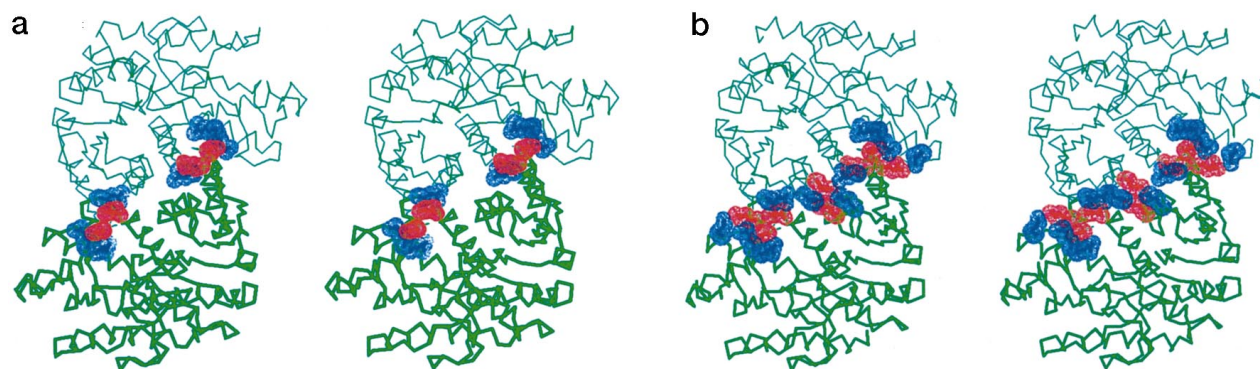


FIG. 6. Stereodiagrams showing the difference of intersubunit ion pairs in Aa MDH (*a*) and in Tf MDH (*b*). Subunit A is in *green* with a *thick line*; subunit B is in *green* with a *thin line*; positively charged residues are in *blue*; and negatively charged residues are in *red*. Some residues have not been labeled for clarity.

activity at low temperatures. Recent comparative studies of citrate synthase from Antarctic bacterial strain DS2-3R and its hyperthermophilic counterpart have shown that an overall average main chain B-factor was much lower in psychrophilic citrate synthase compared with that of hyperthermophilic enzyme (26). However, the small domain in psychrophilic citrate synthase showed more flexibility compared with the large domain, and this difference is more significant in the psychrophilic enzyme than that of its hyperthermophilic counterpart (26). Thus, the domain movement of citrate synthase for enzymatic catalysis upon substrate binding at low temperature is more favorable in psychrophilic citrate synthase. The hydrogen exchange experiments also show evidence for an enhanced rigidity of thermophilic proteins as compared with those from mesophilic proteins (27).

Electrostatic Potential—One of the most remarkable differences between the structures of Aa MDH and Tf MDH is their charge distributions in the accessible surface (28). As seen in Fig. 5, the surface around the NADH binding region in Tf MDH is dominated by negative potentials, whereas that in Aa MDH has significantly weaker negative potentials around the corresponding region. The differences in the position of basic residues of the surface loop comprising residues 91–100 (Arg⁹¹ and Lys⁹² and Lys¹⁰⁶ in Tf MDH/Arg⁹³, Arg⁹⁵, and Lys¹¹⁰ in Aa MDH) results in the different charge distributions within this loop (Fig. 5). The oxaloacetate binding regions in each MDH also show some discrepancies in charge distribution. The oxaloacetate binding region of Aa MDH has more basic regions compared with Tf MDH, since Arg¹⁶⁵, His¹⁹⁰, and Lys²²⁸ are present in Aa MDH, whereas Arg¹⁶¹, His¹⁸⁶, and Gln²²⁸ are in the equivalent region in Tf MDH.

The increased positive potential at and around the oxaloac-

TABLE III
Comparisons of ion pairs, hydrogen bonds, and surface area of two MDHs

The number of ion pairs and hydrogen bonds in Tf MDH have been analyzed from a subunit B. The distance range is 2.2–4.0 Å for an ion pair and 2.2–3.5 Å for a hydrogen bond. All the values of Tf MDH are calculated using the subunit B of Tf MDH structure (accession code 1 bmd of the Protein Data Bank).

	Aa MDH	Tf MDH
No. of intrasubunit ion pairs/subunit	12	8
No. of intrasubunit ion pairs/residue	0.04	0.03
No. of intersubunit ion pairs in dimer (buried/total)	4/6	5/10
No. of intrasubunit hydrogen bonds/subunit	813	800
No. of intersubunit hydrogen bonds in dimer	46	56
Accessible surface area of a subunit (Å ²)	13925.5	14318.9
Buried surface area of dimer (Å ²)	3048.7	3165.0
Total		
Hydrophobic	1937.3	1988.3
Polar	553.2	438.5
Charged	558.2	738.2
No. of the completely buried atoms in a subunit	1277	1253
Fraction	0.52	0.50
No. of the completely buried atoms in the dimer	2680	2577
Fraction	0.54	0.53
Cavities/subunit	8	8

etate binding site and the significantly decreased negative surface potential at the NADH binding region in Aa MDH may facilitate the interaction of a negatively charged substrate toward the surface of the enzyme and may increase the catalytic

efficiency at low temperature.

Thermolability—It has been suggested that high flexibility of an enzyme is tightly correlated to the increased thermolability of the enzyme. Thus, we have analyzed the several factors that could contribute to enzyme stability. These include the number and location of proline/glycine residues and the number of inter- and intrasubunit ion pairs, hydrogen bonds, buried surface areas, and cavities (Table III).

The numbers of glycine and proline residues are very similar in both MDHs, and the positions of these residues are highly conserved in Aa MDH and Tf MDH (Fig. 1a).

While the numbers of Asp, Lys, and His residues are similar, Tf MDH has significantly more Glu and Arg than Aa MDH. Despite such differences, Tf MDH has the same number of intrasubunit ion pairs compared with those of Aa MDH (Table III). Also, an equal number of intrasubunit ion pair networks are found in Aa MDH (Arg²⁴–Asp²⁹–Lys³³, Glu³¹⁹–Arg¹⁰¹–Glu³²⁰) and in Tf MDH (Arg²²–Glu²⁷–Lys³¹, Glu²⁵¹–Arg¹⁵⁶–Asp²⁵⁵). However, Aa MDH has about half the number of intersubunit ion pairs as Tf MDH (Fig. 6). In addition, only three residues, A-Arg¹⁶⁵, B-Asp⁶², and A-Arg²²⁹ (A and B represent each subunit) form ion pair networks, whereas five residue ion pair networks (B-Lys¹⁶⁸, A-Glu⁵⁷, B-Arg²²⁹, A-Asp⁵⁸, and B-Arg¹⁶¹) are observed in Tf MDH.

Ion pairs have emerged as a critical force in stabilizing hyperthermophilic enzymes (29–31). However, the relative importance of intra- or intersubunit ion pairs are still unclear. Also, the contribution of ion pairs to the stability of general proteins other than hyperthermophilic proteins requires further analyses. Nevertheless, the formation of an ion pair network is known to be important to the protein stability. The decreased number of intersubunit ion pairs and ion pair networks is probably one of the major forces in the thermolability of Aa MDH. Recent comparative studies of psychrophilic citrate synthase and its hyperthermophilic counterpart reveal that the psychrophilic enzyme has more intrasubunit and fewer intersubunit ion pairs, emphasizing the importance of intersubunit ion pairs and agreeing with our present analyses (26).

The numbers of hydrogen bonds in both MDHs show similar patterns of ion pairs; Aa MDH has more intrasubunit hydrogen bonds, whereas more intersubunit hydrogen bonds are found in Tf MDH.

The Aa MDH subunit has slightly lower accessible surface area compared with a subunit of Tf MDH (Table III). Aa MDH dimer has 116 Å² of less buried surface area compared with that of Tf MDH. Considering that each square Å has about 25 cal/mol of energy gain, the decreased buried surface area of Aa MDH provides an ~2.9-kcal loss. The more significant difference is found in the nature of the buried surface area in each MDH. While the hydrophobic character is similar in both enzymes, the portion of charged residues in the buried surface area is remarkably smaller in Aa MDH (28%) compared with that of Tf MDH (37%). The increased charged character of the buried surface interface in Tf MDH results in the increased number of intersubunit ion pairs and charged polar group interactions. It has been proposed that the increased number of buried ion pairs in the protein interfaces could contribute to protein stability unlike those present in the core of a protein because of the differences in the surrounding environment and desolvation energy (32). Thus, slightly decreased buried surface area and a smaller portion of charged residues in dimeric interface may contribute to the increased thermolability of Aa MDH.

The number of cavities in both MDHs is the same, and the size of the cavities was very similar (33).

Conclusion

In this paper, we have reported the isolation and biochemical characterization of a MDH from the psychrophilic bacterium, *A. arcticum*, as well as three x-ray structures of Aa MDH. The psychrophilic MDH shows some interesting features: (i) it has 2–3-fold higher k_{cat}/K_m values compared with a mesophilic MDH at a temperature range of 4–10 °C; (ii) its primary structure is highly similar to that of a thermophilic MDH from Tf MDH; and (iii) Aa MDH shows significantly increased thermolability compared with Tf MDH.

Our comparative studies of MDHs from a psychrophile and a thermophile point out three important factors for efficient catalysis by a psychrophilic MDH at low temperatures: (i) an increased relative flexibility at and near the active site region of Aa MDH; (ii) more positive potential in the surface around the oxaloacetate binding site and decreased negative potential around the NADH binding site compared with Tf MDH; and (iii) an increased thermolability of Aa MDH, which is largely contributed by the significantly decreased intersubunit ion pairs and buried surface area in the dimer.

REFERENCES

- Feller, G., Narin, E., Arpigny, J. L., Aittaleb, M., Baise, E., Genicot, S., and Gerday, C. (1996) *FEMS Microbiol. Rev.* **18**, 189–202
- Feller, G., and Gerday, C. (1997) *Cell. Mol. Life Sci.* **53**, 830–841
- Davail, S., Feller, G., Narinx, E., and Gerday, C. (1994) *J. Biol. Chem.* **269**, 17448–17453
- Feller, G., Payan, F., Theys, F., Qian, M., Haser, R. R., and Gerday, C. (1994) *Eur. J. Biochem.* **222**, 441–447
- Gerike, U., Danson, M. J., Russell, N. J., and Hough, D. W. (1997) *Eur. J. Biochem.* **248**, 49–57
- Tsigos, I., Velonia, K., Smonou, I., and Bouriotis, V. (1998) *Eur. J. Biochem.* **254**, 356–362
- Goldman, A. (1995) *Structure* **3**, 1277–1279
- Danson, M. J., and Hough, D. W. (1997) *Struct. Comp. Biochem. Physiol.* **117A**, 307–312
- Frolow, F., Harel, M., Sussman, J. L., Mevarech, M., and Shoham, M. (1996) *Nature Struct. Biol.* **3**, 452–458
- Herbert, R. A. (1992) *Trends Biotechnol.* **10**, 395–402
- Jordan, D. C., and McNicol, P. J. (1979) *Can. J. Microbiol.* **25**, 947–948
- Goward, C. R., and Nicholls, D. J. (1994) *Protein Sci.* **3**, 1883–1888
- Kelly, C. A., Nishiyama, M., Ohnishi, Y., Beppu, T., and Birktoft, J. J. (1993) *Biochemistry* **32**, 3913–3922
- Hall, M. D., Levitt, D. G., and Banaszak, L. J. (1992) *J. Mol. Biol.* **226**, 867–882
- Hall, M. D., and Banaszak, L. J. (1993) *J. Mol. Biol.* **232**, 213–222
- Gleason, W. B., Fu, Z., Birktoft, J. J., and Banaszak, L. J. (1994) *Biochemistry* **33**, 2078–2088
- Birktoft, J. J., Rhodes, G., and Banaszak, L. J. (1989) *Biochemistry* **28**, 6065–6081
- Letherbarrow, R. J. (1987) *ENZFITTER: A Nonlinear Regression Data Analysis Program for the IBM PC/PS 2*, Elsevier Biosoft, Cambridge, United Kingdom
- Otwinowski, Z., and Minor, W. (1997) *Methods Enzymol.* **276**, 307–326
- Brunger, A. T., Kuriyan, J., and Karplus, M. (1987) *Science* **235**, 458–460
- Sacks, J. S. (1988) *J. Mol. Graphics* **6**, 224–225
- Engh, R. A., and Huber, R. (1991) *Acta Crystallogr. Sec. A* **47**, 392–400
- Abad-zapatero, C., Griffith, J. P., Sussman, J. L., and Rossman, M. G. (1987) *J. Mol. Biol.* **198**, 445–467
- Dunn, C. R., Wilks, H. M., Halsall, D. J., Atkinson, T., Clarke, A. R., Muirhead, H., and Holbrook, J. J. (1991) *Philos. Trans. R. Soc. Lond-Biol. Sci.* **332**, 177–184
- Silverstein, E., and Sulebele, G. (1969) *Biochemistry* **8**, 2543–2550
- Russell, R. J. M., Gerike, U., Danson, M. J., Hough, D. W., and Taylor, G. L. (1998) *Structure* **6**, 351–361
- Bonisch, H., Backmann, J., Kath, T., Naumann, D., and Schafer, G. (1996) *Arch. Biochem. Biophys.* **333**, 75–84
- Nicholas, A., Sharp, K. A., and Honig, B. (1991) *Proteins* **11**, 281–296
- Lim, J.-H., Yu, Y. G., Han, Y. S., Cho, S.-J., Ahn, B.-Y., Kim, S.-H., and Cho, Y. (1997) *J. Mol. Biol.* **270**, 259–274
- Yip, K. S. P., Stillman, T. J., Britton, K. L., Artymiuk, P. J., Baker, P. J., Sedelnikova, S. E., Engle, P. C., Pasquo, A., Chiaraluce, R., Consalvi, V., and Rice, D. W. (1995) *Structure* **3**, 1147–1158
- Korndorfer, I., Steipe, B., Huber, R., Tomschy, A., and Jaenicke, R. (1995) *J. Mol. Biol.* **246**, 511–521
- Xu, D., Lin, S. L., and Nussinov, R. (1997) *J. Mol. Biol.* **265**, 68–84
- Kleywegt, G. J., and Jones, A. T. (1994) *Acta Crystallogr. Sec. D* **50**, 178–185